Materials and Structures (2023) 56:148
https://doi.org/10.1617/s11527-023-02234-5

ORIGINAL ARTICLE

Effects of anobiid damage on shear strength parallel to the grain in single step joints

Daniel F. Lima · Jorge M. Branco · João Parracha · José S. Machado · Lina Nunes

Received: 10 March 2023 / Accepted: 28 August 2023 / Published online: 13 September 2023

Abstract Traditional carpentry joints can be found worldwide in many timber truss structures connecting rafter and tie beam. One failure mode of this connection result from shear in the tie beam beyond the notch either due to bad design or deterioration. In this article, the reduction in shear strength of Single Step Joints (SSJ) resulting from biological attack by anobiids was analysed. For this purpose, tests were carried out in non-degraded scots pine (*Pinus sylvestris* L.) specimens (reference) and compared to artificially degraded specimens with three different levels of degradation. The reduction of shear resistance was analysed in relation to the density of holes drilled during the degradation simulation, the loss of mass, and the reduction of the shear-resistant area. At lower degradation levels, no significant reduction in shear strength was observed. On the other hand, the linear regression shows a trend of resistance reduction with increasing degradation. Despite the relatively low coefficient of determination ($r^2 = 0.25$), the parameter that best correlated with the residual strength was the reduction in the shear-resistant area.

Keywords Timber · Single Step Joint · Biological degradation · Anobiid infestation · Residual shear strength

1 Introduction

Wood has reemerged in the construction industry as a structural material, not only due to its sustainable

D. F. Lima · J. M. Branco
ISISE, University of Minho, Campus de Azurém, 4800-058 Guimarães, Portugal
e-mail: daniel.asmf.lima@gmail.com

J. M. Branco
e-mail: jbranco@civil.uminho.pt

J. Parracha · J. S. Machado · L. Nunes (✉)
National Laboratory for Civil Engineering, 1700-066 Lisbon, Portugal
e-mail: linanunes@lnec.pt

J. Parracha
e-mail: jparracha@lnec.pt

J. S. Machado
e-mail: saporiti@lnec.pt

J. Parracha
CERIS–Civil Engineering Research and Innovation for Sustainability, Instituto Superior Técnico, University of Lisbon, 1049-001 Lisbon, Portugal

L. Nunes
cE3c—Centre for Ecology, Evolution and Environmental Changes/Azorean Biodiversity Group/CHANGE–Global Change and Sustainability Institute, University of Azores, 9700-042 Azores, Portugal

appeal, but also for the increased awareness related to the conservation and preservation of the built heritage.

As a natural organic material, wood is subject to biological degradation, where the main agents are fungi and insects. For the biodegradation process activation, a series of factors that contribute to the establishment of the agents must occur for a certain period, such as favourable temperature and relative humidity, the presence of oxygen, moisture content or relevant nutrients.

Although fungal decay can cause severe damage to wood, it tends to be localized inside buildings, while insects usually cause more extensive and generalized damage to the structure. Regarding the degradation caused by insects, the wood-boring beetles (Coleoptera) and termites (Blattodea, Termitoidae) are responsible for most of the problems in older structures, especially in temperate climate countries, such as southern European countries [1].

The assessment of degraded timber elements begins with a visual inspection, aiming to correctly identify the degraded zones, the responsible insects, the wood species, and its quality. This process is primordial to attain the correct diagnosis and intervention strategies [2, 3]. The size and shape of the tunnel, the type of detritus left behind in the tunnel (frass) and the exit holes made by the emerging adults are all characteristics of the species of beetle. Some timbers are more susceptible to attack than others and generally the heartwood is much more resistant than the sapwood [4].

In general, the boring beetles' degradation is considered either by reducing the element cross section or by assuming reduced mechanical properties for the initial cross sections [2, 5, 6]. However, the more or less diffuse attack of these insects turns the evaluation of the damage intensity more difficult [7]. The lack of knowledge, combined with the difficulty in assessing the extent and severity of damage in situ, is responsible for many unnecessary replacements of structures that could be subjected to curative treatments and/or reinforcements, leading to an increase in the rehabilitation cost and reducing the service life of these structures.

In this context, timber roofs represent a great challenge, being common to find elements and joints degraded by insects and fungi due to their constant contact with the supporting masonry [8]. Under normal conditions, direct contact between timber elements and the supporting masonry, which can be made of stone or brick, should not be a problem. However, one of the most recurrent pathologies in masonry is the presence and proliferation of moisture [9], contributing to the occurrence of favorable conditions for the activation of the deterioration process.

Timber roofs traditionally are composed by trusses using carpentry joints. Among the traditional carpentry joints, which, over time, have developed numerous techniques and geometries, the Single Step Joint is commonly found due to its simple configuration, which implies simpler cuts for carpenters [10]. Moreover, this is the joint most used to connect the rafter to the tie-beam when the later finds the masonry support.

In the existing literature, it is possible to find some studies with the objective to quantify the impact of anobiids on timber structures, e. g. [11–18]. During the visual inspection of a structure, the intensity of the infestation is usually evaluated by the examination of the surface appearance. However, studies like[14, 16] revealed that the internal holes intensity tends to be greater than that of the surface holes, leading to a sub estimation of the degradation level, thus exposing the relevance of the development of techniques to correctly estimate the amount of wood consumed by the beetles and its impact on the structural safety.

Parracha et. al. [14] proposed a semi-destructive assessment method that correlates the residual strength of maritime pine (*Pinus pinaster* Ait.) structural elements degraded by anobiids with the screw pullout resistance. In Parracha et. al. [16], the difficulty in quantifying the degradation caused by wood boring insects is reported, as micro-X-ray computed tomography images showed that the classification of degradation from the surface emergency holes does not reliably correspond to the loss of material inside the elements. Verbist et. al. [15], performing compression tests perpendicular to the grain in chestnut (*Castanea sativa* Mill.), observed a reduction in the compression strength perpendicular to the grain and corresponding modulus of elasticity with the presence of beetle attack. However, it was clear the difficulty in establishing correlations between the loss of material caused by insect attack and the mechanical resistance, mostly due the diffuse damage caused by the insects and the difficulty in quantifying the level of degradation [15].

Degl'Innocenti et al. [17] conducted an analysis and testing of timber elements degraded by insects, retrieved from a nineteenth-century building. The study yielded reduction coefficients ranging from 1.7 to 5.0, which were further validated through numerical models. However, the authors emphasized that the procedure was effective only for timber elements without localized major defects or anomalies, such as woodworking or internal decay. Finally, Nocetti et al. [18] investigated the feasibility of utilizing drilling resistance measurements to assess the degradation depth caused by insects in solid wood structural elements. They established an automatic test routine to facilitate the process. Although their study showed promising results, the drilling profiles were not highly accurate in assessing the degradation caused by anobiid insects.

In this context, this paper aims to verify the reduction in the shear strength parallel to the grain in Single Step Joints degraded by wood boring insects from the *Anobiidae* family, namely *Anobium punctatum* De Geer (known as woodworm or common furniture beetle). The insect attack was artificially simulated in tie beams considering three different levels of deterioration. Finally, a correlation was established between the loss of mechanical properties via shear strength parallel to the grain and the level of degradation.

2 Materials and methods

An experimental campaign workflow was defined, Fig. 1. The first step comprised the selection of scots pine timber pieces to produce Single Step Joints (SSJ), see Sect. 2.1. At a second step a simulation deterioration due to a woodboring beetle (e.g. *A. punctatum*) was performed in some tie beams, see Sect. 2.2. A third step comprised the mechanical testing of undamaged SSJ and damaged (three levels of deterioration) SSJ, see Sect. 2.3. Finally, the influence of degradation on the mechanical strength of the Single Step Joint was analysed, seeking to correlate loss of mechanical properties with the level of degradation.

2.1 Specimens and SSJ

The SSJ specimens with structural dimensions used for the destructive tests were made of scots pine (*Pinus sylvestris* L.), with the front notch perpendicular to the tie beam grain ($\alpha = 0°$) and a skew angle between the tie beam and the rafter of 30° ($\beta = 30°$), Fig. 2.

To assure wood quality control and verify the compliance with EN 338 [19] for the strength class, a comprehensive visual grading process was employed. The assessment involved an initial photographic survey, followed by the implementation of the UNE 56544 [20] procedure. All defects and distinctive characteristics specified in the relevant standard were meticulously identified and measured, encompassing elements such as knots, resin pockets, fissures, wane, biological damage, distortions, and width of the annual rings, among others.

Before carrying out all the procedures of the experimental campaign, the specimens were stored in a climatic chamber at a constant temperature of $20 \pm 1°C$ and a relative humidity of $60 \pm 5\%$ until mass stabilization (i.e., difference $\leq 0.1\%$ between consecutive measurements) (EN 13183 [21]]). Under these climatic conditions, the equilibrium moisture content of the wood should be approximately 12% [22].

Moisture content (w) and density (ρ_w) were determined following the procedures of EN 13183 [21] and NP 616 [23], respectively. These parameters were measured right after the execution of the tests. Samples for moisture content were collected from the cross section as close as possible to the failure, as recommended in EN 408 [24]. Additionally, the density values were corrected to a 12% moisture content value (ρ_{12}).

2.2 Artificial degradation

The simulation of degradation was performed by open holes in the direction parallel to the grain on the tie beam-end element. For that purpose, it was used a hand-held electric drill machine and a ∅2 mm drill bit.

The dimension of the perforated galleries was approximately 2 mm in diameter and 100 mm in length since the furniture beetle normally makes circular galleries of 1–3 mm in diameter [22], and the length of the tie beam-end is 100 mm (zone subject to shear tension).

Prior simulations of artificial degradation on $100 \times 100 \times 100$ mm^3 specimens showed that drilling always resulted in deviations caused by the large

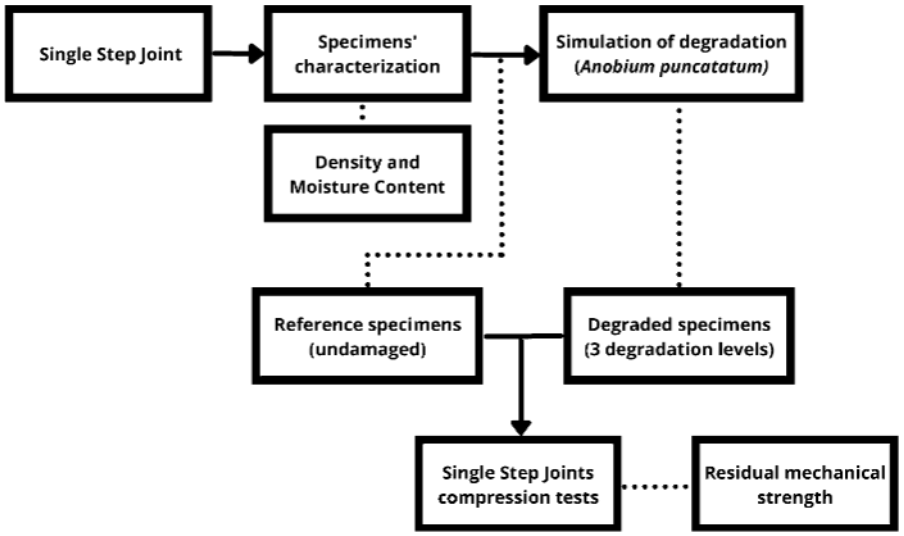

Fig. 1 Experimental campaign workflow

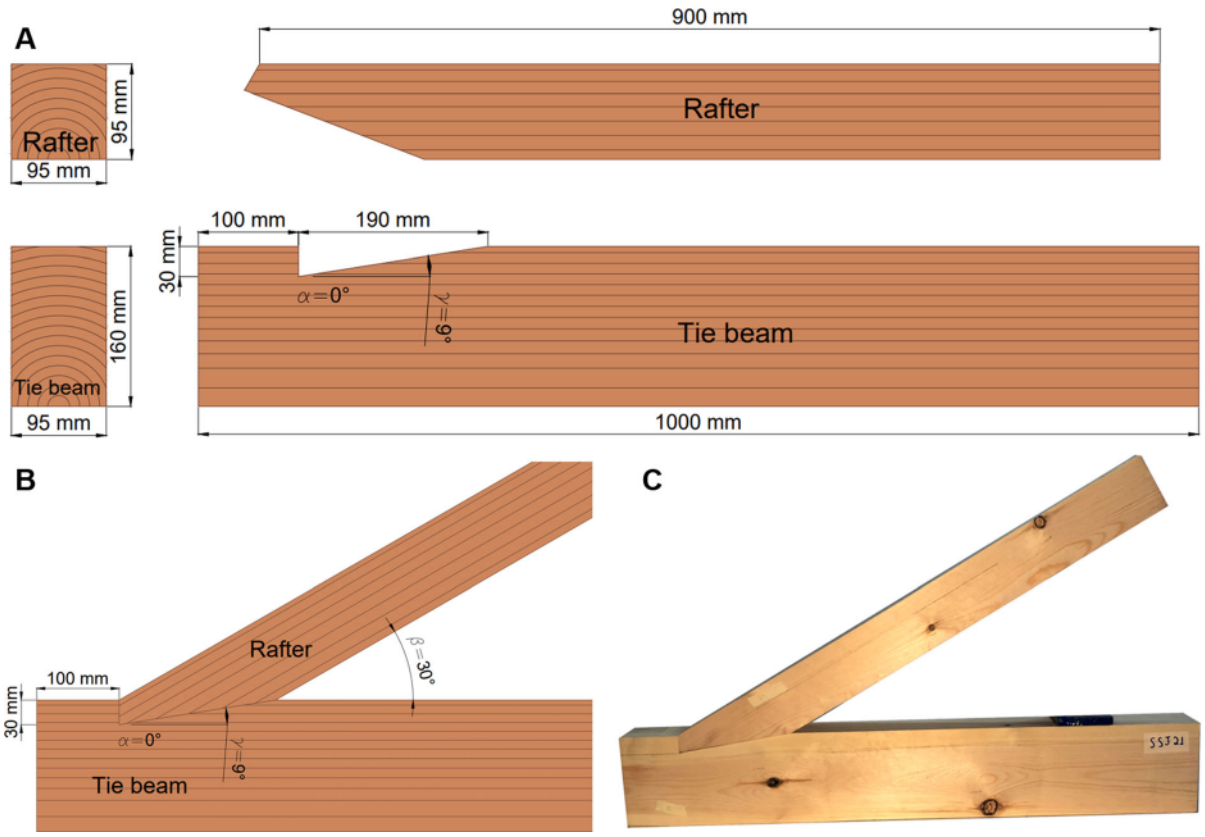

Fig. 2 Single step joint specimen: **A** dimensions; **B** geometry; **C** specimen

length and small diameter of the drill, regardless of being attempted in straight rows. As a result, the artificially holes exhibited a random distribution along the galleries' path. Furthermore, in a previous study [25] three drilling patterns were considered (i.e., random, orthogonal and quincunx) to artificially

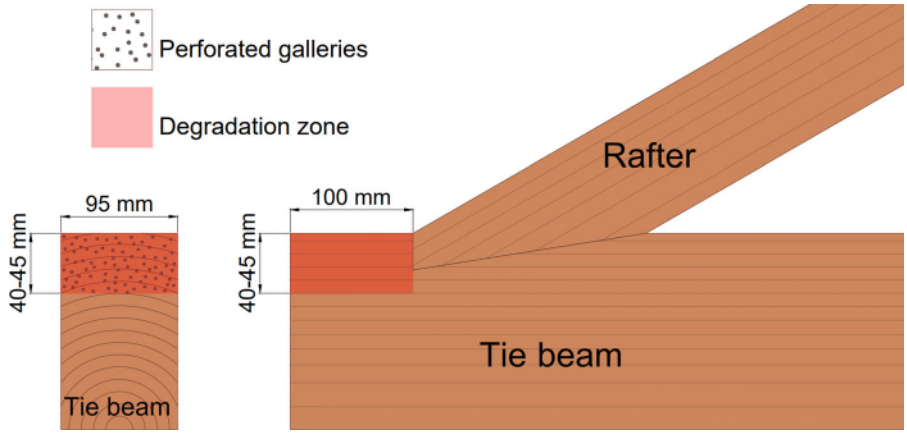

Fig. 3 Simulation of the degradation zone on the Single Step Joints specimens

simulate anobiid degradation in the direction parallel to the grain of small pine wood specimens. Results showed no significant differences in compression parallel to the grain considering the different drilling patterns.

Figure 3 shows the degradation zone. This configuration was adopted because of the objective of this study, which aims to analyze the loss of shear resistance. The analysis of the shear resistance was chosen based on its brittle behaviour, which turns this failure more critical than the crushing failure.

Three different levels of degradation were adopted, varying the density of perforated galleries (number of holes/cm^2). The simulation sought to achieve realistic degradation levels compatible with degraded structures found in situ. Verbist et. al. [15], when quantifying the density loss resulting from woodworm attacks on chestnut beams, obtained values between 2.44 and 14.69%. Meanwhile, Parracha et. al. [14] obtained values between 9.2 and 21.9% from the analysis of μ-XCT images of samples taken from maritime pine beams. Therefore, the densities of galleries were defined by previous simulations on small specimens carried out by Lima [26]. The densities adopted in this study were correspondents to 1.67, 3.33 , and 4.00 holes/cm^2, called ML-I, ML-II, and ML -III, with expected mass losses of 5.2, 10.5, and 12.6%, respectively. The expected mass loss was calculated considering the material lost from the dimensions of the galleries and the drilling density.

The quantification of artificial degradation was carried out by measuring the mass of the specimen before and after drilling the galleries, obtaining the loss of mass relative to the degraded zone. Additionally, the reduction of the shear resistant surface was measured for each specimen after the compression test.

2.3 Single step joints tests

After performing the artificial simulation of wood degradation, the joint specimens were tested under increasing axial compression on the rafter until failure, Fig. 4. Under this type of stress, two possible failure modes are expected, namely, crush by compression parallel to the grain on the front notch surface and failure by shear parallel to the grain on the tie beam-end [10]. Verbist et al. [10], when conducting compression tests in single step joints in order to compare experimental results with the design equations usually found in the literature, concluded that in joints with low rafter skew angle ($\beta = 30°$), with a reduced ratio between the heel depth and the shear length ($lv/tv \leq 6$) and with the front notch perpendicular to the grain of the tie beam, the failure tends to occur by shear parallel to the grain in the tie beam-end. Therefore, the geometry of the specimens used in this experimental campaign complied with those rules to induce failures by shear parallel to the grain (see Sect. 2.1).

The test was conducted until failure through the application of a normal load (N_{Rafter}) on the rafter. The normal load was applied by a hydraulic actuator controlled by displacement with a speed of 0.01 mm/s and measured by a 100 kN load cell. The load resulted in compressive stresses on the surfaces of the joint (i.e., compression parallel to the grain on the Front

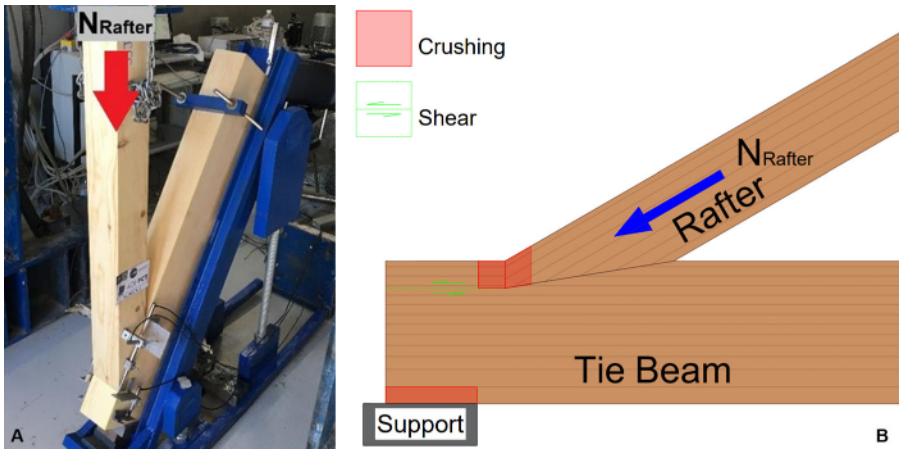

Fig. 4 Compression test of the Single Step Joints. **A** Test setup; **B** Illustration of possible failure modes (adapted from [10, 12])

Notch and perpendicular to the grain on the Bottom Notch) and shear forces on the tie beam-end (Fig. 4). Additionally, the SSJ front notch and actuator displacements were measured by LVDTs (Linear Variable Differential Transformer).

40 specimens were tested: 4 undamaged specimens (i.e., reference) and 12 specimens for each of the three levels of degradation considered, totaling 4 distinct groups (Table 1). The shear strength parallel to the grain (f_v) was calculated using Eq. 1.

$$f_v = \frac{N_{\text{rafter}} \times \cos\beta}{l_v \times b} \quad (1)$$

where N_{rafter} is the compression force registered by the actuator at the failure moment, β is the skew angle between the rafter and tie beam, l_v is the shear length, and b is the specimen width.

3 Results and discussion

As aforementioned the geometry of the Single Step Joint specimen was defined to induce failure by shear parallel to the grain in the tie beam-end, based on the experimental results obtained by Verbist et al. [10]. Thus, all 40 specimens presented shear failure with no crushing parallel to the grain at the front notch or perpendicular to the grain at the bottom notch (Fig. 5).

Table 2 presents the results obtained in the characterization tests (namely moisture content and density adjusted for a moisture content of 12%), as well as the results obtained in the degradation simulation (both in terms of mass loss and shear resistant area reduction).

The moisture content average values between 12.6 and 12.8% are compatible with what indicates the hygrothermal equilibrium curve exposed in [22] for the adopted environmental conditions. Regarding the density of the specimens, average values between 493 and 529 kg/m^3 were obtained.

Gilfillan & Gilbert [11] reported the difficulty in achieving high levels of degradation from the manual drilling of galleries to simulate the wood boring insects, from the Anobiidae family, in its larval state. In the same way, from Table 2, it is possible to infer that the simulation of the degradation did not reach the expected mass loss values, obtaining, on average, 3.2, 6.6, and 6.7%, for the groups SSJ_ML-I, SSJ_ML-II, and SSJ_ML-III, respectively. The amount of sawdust that remains inside the drilled galleries and the deviations suffered by the drill during the process (which led the holes to encounter during the course and the consequent reduction of exit holes) (Fig. 6) are factors that may have contributed to the lower mass loss values obtained.

Regarding the shear strength, firstly it was verified that the distribution of the results fit the normal distribution through the Shapiro–Wilk test ($p = 0.14$). Next, the test results were analyzed according to their level of degradation, considering the quantification of degradation in terms of density of perforated galleries, mass loss, and reduction of the shear resistant section area.

Table 1 Summary of the distribution of the specimens into the different degradation zones and levels for the Single Step Joint tests

Group name	Number of specimens	Degradation level (holes/cm^2)
SSJ_REF	4	–
SSJ_ML-I	12	1.67
SSJ_ML-II	12	3.33
SSJ_ML-III	12	4.00

SSJ–Single Step Joint; REF–Reference; ML-I–Mass Loss I (Degradation level I); ML-II–Mass Loss II (Degradation level II); ML-III–Mass Loss III (Degradation level III)

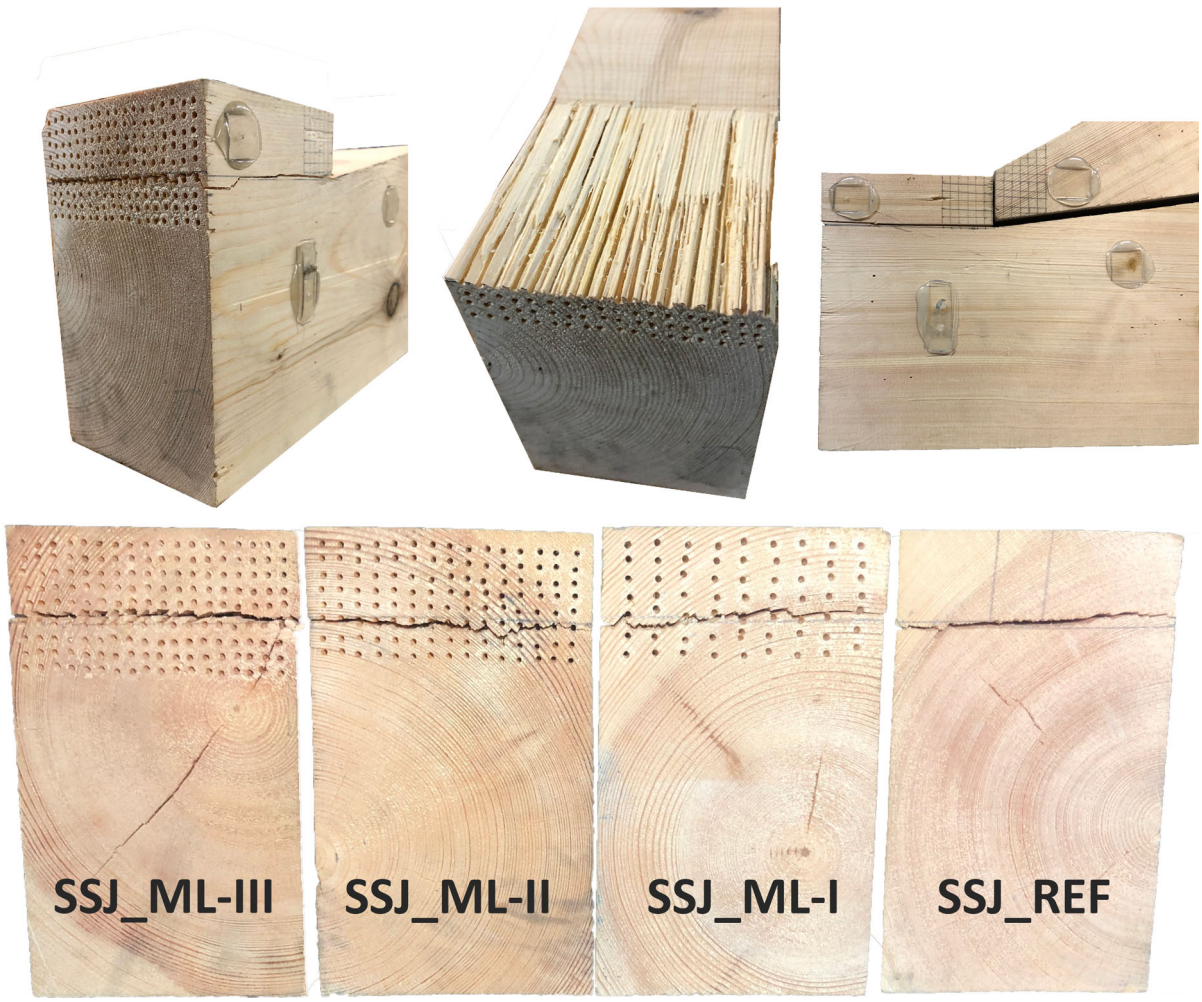

Fig. 5 Characteristic shear failure on the tie beam-end observed in all Single Step Joints tested under compression

3.1 Shear strength as function of drilling density

As previously mentioned, drilling densities equivalent to 1.66, 3.33, and 4.00 holes/cm^2 were adopted, corresponding to groups SSJ_ML-I, SSJ_ML-II, and SSJ_ML-III, respectively. Figure 7A shows the bar chart that graphically represents the shear strength mean values and the respective standard deviations of the degradation groups. Meanwhile, Figs. 7B, C and D show the comparison between the sound (SSJ_REF)

Table 2 Summary of the results obtained from the Single Step Joints characterization tests and degradation simulation

Group		SSJ_REF	SSJ_ML-I	SSJ_ML-II	SSJ_ML-III
N°		4	12	12	12
w[%]	$\overline{X}$	12.8	12.6	12.6	12.6
	σ	0.8	0.8	0.9	0,9
	C.V	6.4%	6.6%	7.6%	7.4%
ρ_{12}[kg/m^3]	$\overline{X}$	529	514	511	493
	σ	26	50	41	52
	C.V	4.9	9.8	7.9	10.6
ML [%]	$\overline{X}$	0	3.2	6.6	6.7
	σ	0	0.6	1.2	0.6
	C.V	0%	18.8%	18.2%	9.0%
AR [%]	$\overline{X}$	0	7.8	17.8	17.2
	σ	0	3.2	4.2	4.5
	C.V	0%	41.1%	23.8%	25.9%

$\overline{X}$–Average; σ–Standard Deviation; C.V.–Coefficient of variation; w–Moisture Content; ρ_{12}–Density corrected to a 12% moisture content; ML–Mass Loss; AR–shear resistant area reduction

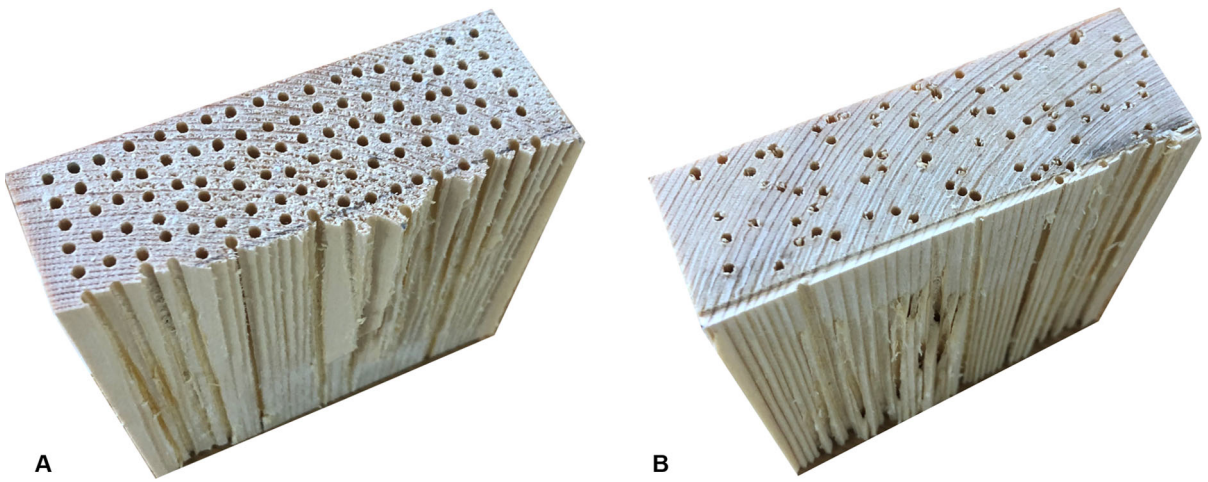

Fig. 6 Simulation of the insect attack in the tie beam-end. **A** Entrance galleries; **B** Exit galleries

and degraded front notch force–displacement curves, and Table 3 shows the mean value and the standard deviation of the maximum compressive force and its respective front notch displacement for each group.

Through the analysis of Fig. 7 and Table 3, it is possible to observe that the group with the lowest level of degradation (SSJ_ML-I) presented superior results (+ 4%, on average) compared to the reference group (SSJ_REF). On the other hand, the higher two levels of degradation showed lower tests results than the reference group (− 10 and − 11%, on average). Therefore, it was carried out a *t*-test for equal means (Welch´s test) to verify the statistical significance of the degradation on the shear resistance. The results of the t-tests are shown in Table 4.

The Welch's test is based on a *t*-value, a critical *t*-value, and a null hypothesis H_0, where a *t*-value higher than the critical one rejects the null hypothesis, indicating a statistically significant difference between the means [27]. Thus, through the analysis of Table 3 is possible to infer that, at the first level of degradation (SSJ_ML-I), the degradation was not enough to cause significant damage to the specimen (*t*-value < critical value) and, in this group, other properties such as density and wood variability were more determinant in the shear strength parallel to the grain. Meanwhile, the

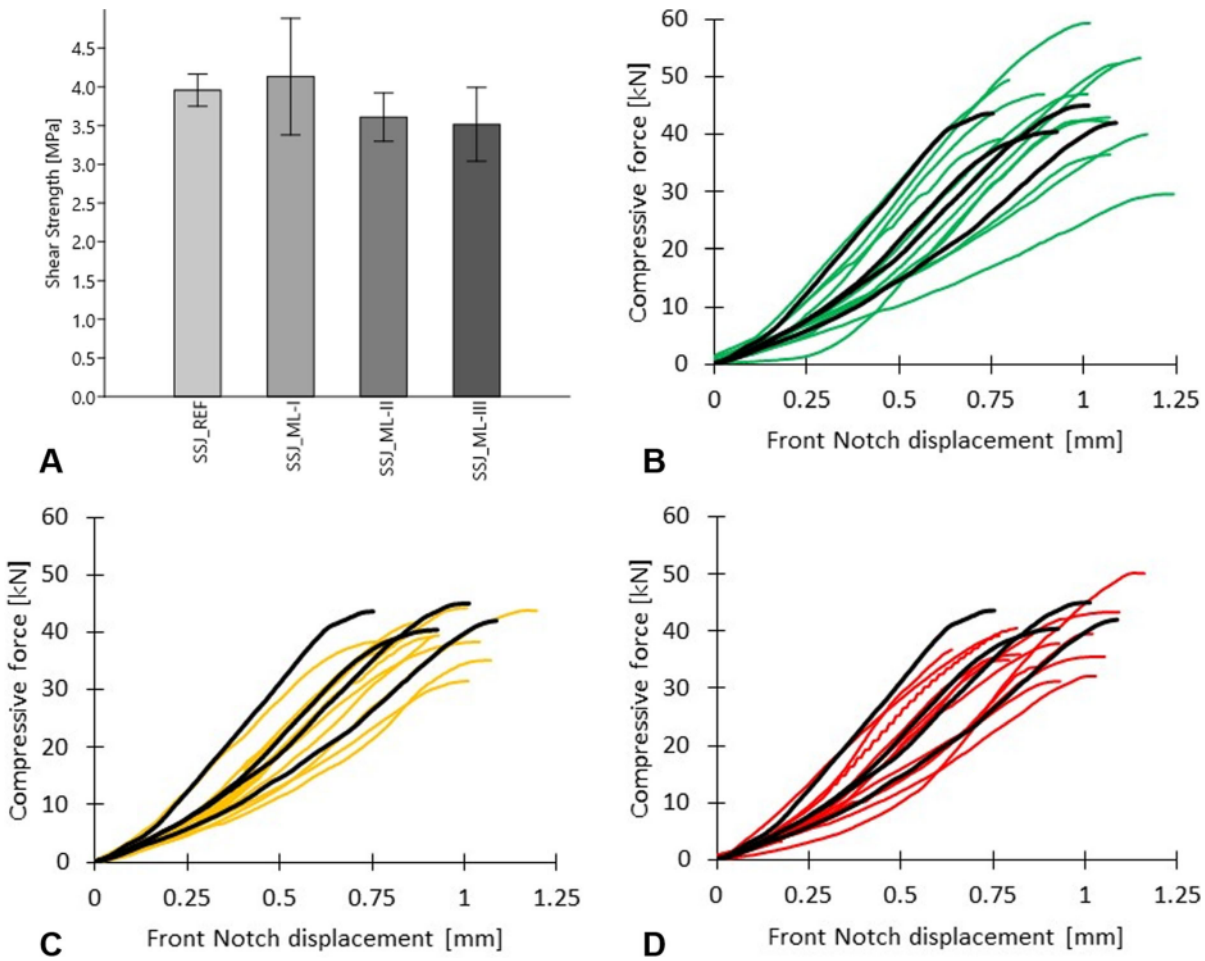

Fig. 7 Results of the Single Step Joint test. **A** Bar chart of the shear strength for each degradation group; **B** Force–displacement graph of the SSJ_REF (black) and SSJ_ML-I (green) specimens; **C** Force–displacement graph of the SSJ_REF (black) and SSJ_ML-II (yellow) specimens; **D** Force–displacement graph of the SSJ_REF (black) and SSJ_ML-III (red) specimens

Table 3 Mean value and the standard deviation of the maximum compressive force and its respective front notch displacement for each group

Group		SSJ_REF	SSJ_ML-I	SSJ_ML-II	SSJ_ML-III
N_{rafter}[kN]	$\overline{X}$	43.4	45.3	39.6	38.6
	σ	2.3	8.2	3.4	5.2
	C.V	5.2%	18.2%	8.7%	13.5%
d[mm]	$\overline{X}$	0.95	1.03	0.94	0.92
	σ	0.15	0.14	0.12	0.15
	C.V	15.6%	13.98%	12.32%	16.48%

$\overline{X}$–Average; σ–Standard Deviation; C.V.–Coefficient of variation; N_{rafter}–Maximum compressive force; d–Front notch displacement

Table 4 Summary of the results of the *t*-tests for equal means (Welch´s test)

		T-value	Critical *t*-value
SSJ_REF	SSJ_ML-I	0.725	2.145
	SSJ_ML-II	2.529	
	SSJ_ML-III	2.574	

other two levels of degradation presented *t*-values higher than the critical, demonstrating the influence of the drilled galleries on the shear resistance of the tie beam-end of the Single Step Joint.

From the tests results, it was possible to establish the correlation between the shear strength, the original density, and the residual density, since it is one of the physical characteristics that better correlates with the wood mechanical properties. The residual density was measured using probes collected from the Tie beam-end heel resulting from the shear failure (Fig. 6). Figure 8 presents the linear correlations between shear strength and density (original and residual) for each degradation group considered.

The coefficients of determination (r^2) presented agrees with the statement that, for lower levels of degradation, the wood density is still predominant in the behavior of the structure and a positive correlation is obtained, Figs. 8a and b. At more advanced degradation levels, the coefficient of determination decreases, and negative linear regression lines are obtained (Figs. 8c and d), indicating that density is no longer the principal independent variable.

Additionally, the significance of the linear regression models was calculated for a 5% level ($p < 0.05$). Of the seven models presented in Fig. 8, only the correlation between shear strength and residual density of the SSJ_ML-I group (Fig. 8b) showed significance at a level of 5% ($p = 0.038$). One should notice that the linear regression shown in Fig. 8a is not significant for a level of 5% ($p = 0.17$) due to the small number of samples since the correlation between the density and the shear strength of undamaged timber has already been proven in several works, for example Denzler & Glos [28] and Gremik & Surini [29]. The calculated significances for the linear regression models reaffirm the analysis of the coefficient of determination carried out above.

3.2 Shear strength as function of mass loss

The mass loss relative to the degraded zone was defined through the mass measurement before and after the degradation simulation, and the correlation between the shear strength and the mass loss was established from these values. Figure 9 presents the scatter plot and the linear regression of the results distinguishing the degradation groups adopted. Since the results exposed in Sect. 3.1 showed no difference in shear strength between the reference group (SSJ_REF) and the group with the lowest level of degradation (SSJ_ML-I), it was decided to consider only the degraded specimens in the linear regression of the results.

Firstly, the significance for a 5% level of the linear regression was verified, obtaining a p-value of 0.036. From the analysis of Fig. 9, it is possible to observe that, despite a relatively low coefficient of determination ($r^2 = 0.12$), the trend line of the linear regression indicates the reduction of the shear strength parallel to the grain with the increase of the degradation.

Additionally, it is possible to observe the difficulty in simulating higher degradation levels, as reported in [11]. The mass losses values of the SSJ_ML-II group presented high variability, with values between 4.9 and 9.0%. On the other hand, the mass losses obtained for the SSJ_ML-III group has lower variability, but contains some lower values than those of the SSJ_ML-II group, despite having a higher drilling density.

3.3 Shear strength as function of effective shear area

To establish the correlation between the effect of the woodworm activity on the reduction of the shear stress area and the shear strength, it was first necessary to evaluate the effective shear area (defined as the area not affected by holes). The quantification of the effective shear area was carried out from photographs taken perpendicular to the shear resistant area, after the test. It was then possible to perform the contour of the areas of interest and, from this contour, to obtain its numerical value, Fig. 10.

Figure 11a presents the scatter plot of the results of the tests in relation to its area reduction and the correlation between the shear strength and the degradation. Firstly, the significance for a 5% level of the linear regression was verified, obtaining a *p* of 0.002.

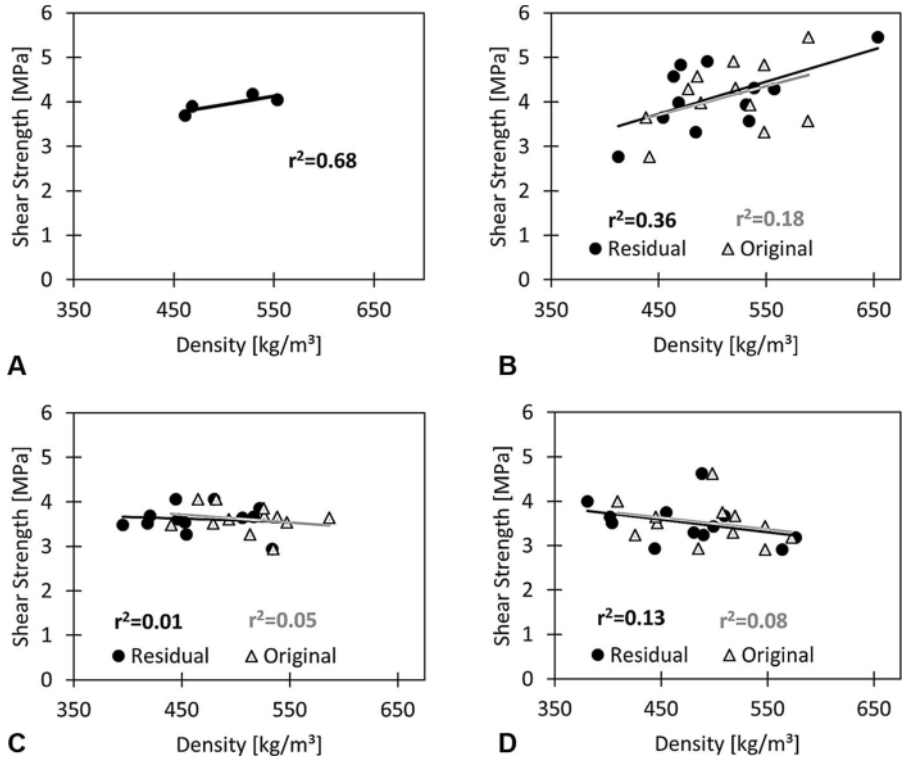

Fig. 8 Correlations between shear strength and density for each degradation level group. **A** SSJ_REF; **B** SSJ_ML-I; **C** SSJ_ML-II; **D** SSJ_ML-III

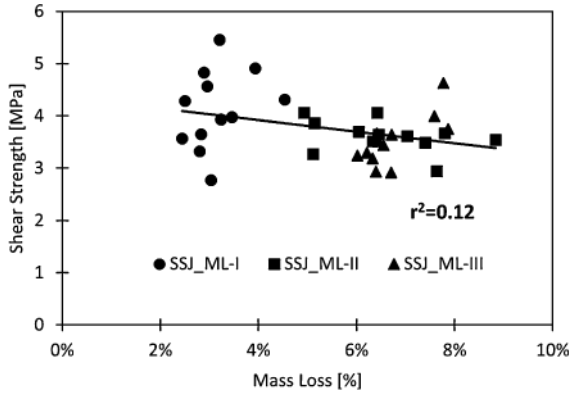

Fig. 9 Correlation between shear strength and mass loss

As noticed when correlated with the mass loss, the regression line presents also in this case a negative slope. In other words, the shear strength tends to reduce according to the increase of degradation. The coefficient of determination obtained was $r^2 = 0.25$, greater than twice the one obtained for mass loss ($r^2 = 0.12$).

In theory, the specimen should show linear variation in shear strength with section variation, where 100% loss of resistant area would result in zero shear strength, and 0% loss of resistant area would result in maximum shear strength. The representation of the theoretical resistance reduction curve from the reduction of the resistant area was inserted in Fig. 11 ($y = -4.45x + 4.45$). It is possible to infer from Fig. 11 that the trend line of the results and the theoretical reduction curve are similar, with only a slight difference in their slope.

Moreover, the design value for the shear strenght according to the recommendations of the Eurocode 5 [30] has been calculated. Eurocode 5 [30] defines the design value of a wood strength property multiplying the characteristic strength value by the modification factor considering duration of load and moisture content (k_{mod}) while dividing by the partial factor for wood properties (γ_M). Based on the recommendations of Eurocode 5 [30], it was considered 1.3 for γ_M and 0.9 for k_{mod}. In this study, the scots pine was classified as C24 strength class, with a characteristic shear

Fig. 10 Quantification of the resistant area reduction

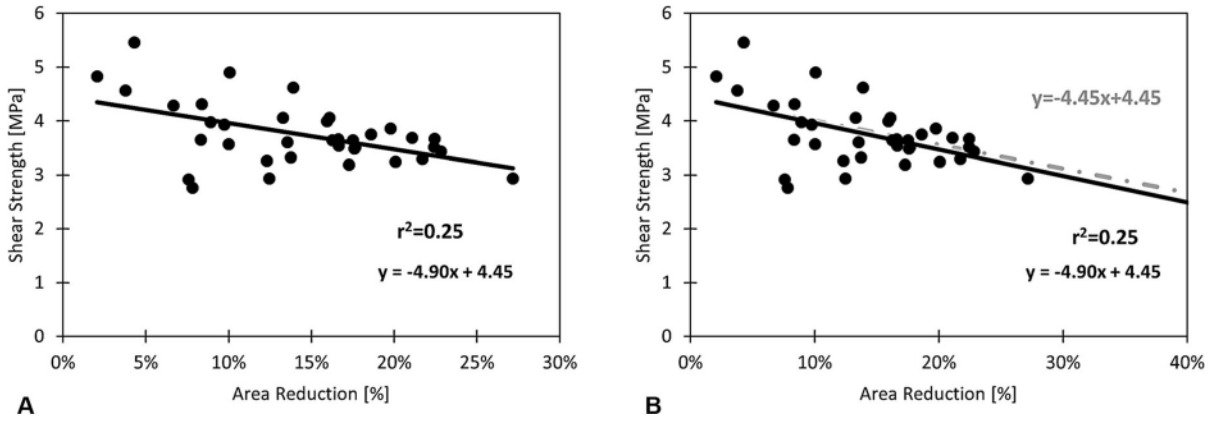

Fig. 11 Correlation between the shear strength and the reduction of the resistant area **A**, and equation of strength reduction according to the reduction of the resistant area **B**

strength of 4.0 MPa [19]. Therefore, the characteristic shear strength ($f_{v,k}$ = 4.0 MPa), and the design strength of 2.8 MPa are represented in Fig. 12.

By the analysis of Fig. 12, it is observed that none of the specimens presented strength below the design value. The results point out that failure can occur for a reduction of the area between 35 and 37%. On the other hand, when considering the characteristic shear strength, some specimens present results lower than 4.0 MPa from 8% of area reduction. Additionally, from 16% of area reduction, all 17 specimens present resistance lower than the characteristic value. Analyzing the Table 1, a 16% of area reduction can correspond to a mass loss around only 6.7%. However, it is necessary to point out that the relatively low coefficient of determination (r^2 = 0.25) and the lack of results for higher levels of degradation makes it necessary to carry out more tests to obtain a more accurate correlation.

4 Conclusions

In this study, it was sought to evaluate the impact of woodworm (common furniture beetle) infestation on the shear strength of Single Step Joints. From the experimental campaign, it was observed a reduction in the shear strength perpendicular to the grain of approximately 10% for the degradation level ML-II (3.33 holes/cm^2) and 11% for the degradation level

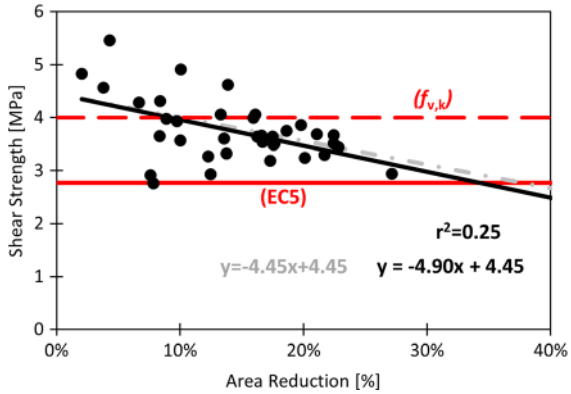

Fig. 12 Correlation between the shear strength and the reduction of the resistant area, equation of strength reduction according to the reduction of the resistant area, characteristic shear strength (C24 [19]), and design value for the shear strenght according to Eurocode 5 [29]

ML-III (4.00 holes/cm^2). On the other hand, statistical analysis (Welch's test) showed no significant difference between the shear resistance of the reference group (SSJ_REF) and lowest level of degradation (SSJ_ML-I, 1.67 holes/cm^2), demonstrating that at lower levels, the degradation caused by this insect has no relevance, and the density and wood quality still govern its mechanical behavior.

Although it is possible to observe the tendency to reduce the resistance with the increase of the degradation level, relatively low coefficients of determination were obtained ($r^2 = 0.12$ for the mass loss correlation and $r^2 = 0.25$ for the area reduction correlation). However, it is fundamental to note that wood is a natural material presenting a high variability in its properties and when considering the biological degradation, the analysis of the material and the correlation between properties become even more complex and difficult. As consequence, it is important to point the need to carry out tests on a large scale and with a higher range of degradation levels than those studied in this work, for an accurate correlation between degradation and decrease of the mechanical properties. On the other hand, it is noteworthy that even for the highest degradation levels achieved here, no specimen showed shear strength below the design strength calculated according to Eurocode 5 [30]. This fact demonstrates that despite being extremely relevant as an initial evaluation and identifying the most critical points to be analyzed, the quantification of degradation from the visual classification of the element surface can often lead to more conservative diagnoses and unnecessary replacements. However, the effects on the shear strength becomes evident when comparing the results with the characteristic value for C24 softwood (Fig. 12).

Therefore, is evident the need to establish new semi/non-destructive methods and validate the existing ones for in situ evaluation of biologically degraded wooden structures, to complement the visual classification and provide a solid basis for engineers and architects to perform an accurate diagnosis to sustain a correct intervention.

Acknowledgments This work is supported by national funds through FCT – Fundação para a Ciência e a Tecnologia within a Ph.D. scholarship within MIT Portugal Program (PRT/BD/152833/2021).

Funding Open access funding provided by FCT|FCCN (b-on).

Declarations

Conflict of interest The authors declare no conflict of interest.

References

1. Eaton RA, Hale MDC (1993) Wood: decay, pests, and protection, 1st edn. Chapman & Hall, London
2. Cruz H, Yeomans D, Tsakanika E et al (2015) Guidelines for on-site assessment of historic timber structures. Int J Archit Herit 9:277–289. https://doi.org/10.1080/15583058.2013.774070
3. Machado JS, Pereira F, Quilhó T (2019) Assessment of old timber members: importance of wood species identification and direct tensile test information. Constr Build Mater 207:651–660. https://doi.org/10.1016/j.conbuildmat.2019.02.168
4. Parracha JL, Duarte S, Faria P, Nunes L (2018) A importância dos insetos de madeira seca na reabilitação de

estruturas de madeira. Construção 2018 - Reabilitar e construir de forma sustentável. Porto, Portugal, pp 771–780
5. UNI 11119:2004. Cultural heritage–Wooden artefacts–Load bearing structures of buildings–On site inspection for the diagnosis of timber members, UNI, Milan
6. EN 17121:2019. Conservation of cultural heritage–Historic timber structures–Guidelines for the on-site assessment of load-bearing timber structures. European Committee for Standardization, Brussels
7. Reinprecht L (2016) Wood deterioration, protection and maintenance. Wiley, Chichester
8. Branco JM, Verbist M, Descamps T (2018) Design of three step joint typologies: review of european standardized approaches. Eng Struct 174:573–585. https://doi.org/10.1016/j.engstruct.2018.06.073
9. Franzoni E (2018) State-of-the-art on methods for reducing rising damp in masonry. J Cult Herit 31:S3–S9. https://doi.org/10.1016/j.culher.2018.04.001
10. Verbist M, Branco JM, Poletti E et al (2017) Single step joint: overview of european standardized approaches and experimentations. Mater Struct. https://doi.org/10.1617/s11527-017-1028-4
11. Gilfillan JR, Gilbert SG (2001) Development of a technique to measure the residual strength of woodworm infested timber. Constr Build Mater 15:381–388
12. Cruz H, Machado JS (2013) Effects of beetle attack on the bending and compression strength properties of pine wood. Adv Mat Res 778:145–151. https://doi.org/10.4028/www.scientific.net/AMR.778.145
13. Brites RD, Neves LC, Machado JS et al (2013) Reliability analysis of a timber truss system subjected to decay. Eng Struct 46:184–192. https://doi.org/10.1016/j.engstruct.2012.07.022
14. Parracha JL, Pereira MFC, Maurício A et al (2019) A semi-destructive assessment method to estimate the residual strength of maritime pine structural elements degraded by anobiids. Mater Struct. https://doi.org/10.1617/s11527-019-1354-9
15. Verbist M, Branco JM, Nunes L (2020) Characterization of the mechanical performance in compression perpendicular to the grain of insect-deteriorated timber. Buildings. https://doi.org/10.3390/buildings10010014
16. Parracha J, Pereira M, Maurício A et al (2021) Assessment of the density loss in anobiid infested pine using x-ray micro-computed tomography. Buildings. https://doi.org/10.3390/buildings11040173
17. Degl'Innocenti M, Nocetti M, Kovacevi VC, Aminti G, Betti M, Lauriola MP, Brunetti M (2022) Evaluation of the mechanical contribution of wood degraded by insects in old timber beams through analytical calculations and experimental tests. Construct Build Mater. https://doi.org/10.1016/j.conbuildmat.2022.127653
18. Nocetti M, Mannucci M, Brunetti M (2023) Automatic assessment of insect degradation depth in structural solid wood elements by drilling resistance measurements. Construct Build Mater. https://doi.org/10.1016/j.conbuildmat.2022.130273
19. EN 338:2016. Stuctural timber - Strength classes. European Committee for Standardization, Brussels
20. UNE 56544:2011. Clasificación visual de la madera aserrada para uso estructural–Madera de coníferas. AENOR, Madrid
21. EN 13183:2012. Moisture content of a piece of sawn timber. European Committee for Standardization, Brussels
22. Cruz H, Jones D, Nunes L (2015) Wood. Materials for Construction and Civil Engineering. Springer, Cham, pp 557–583
23. NP 616:1973. Madeiras. Definição da massa volúmica. Norma Portuguesa, IGPAI, Lisboa
24. EN 408:2010. Timber structures–Structural timber and glued laminated timber–Determination of some physical and mechanical properties. European Committee for Standardization, Brussels
25. Nunes L, Parracha JL, Faria P, Palma P, Maurício A, Pereira MFC (2019) Towards an assessment tool of anobiid damage of pine timber structures. IABSE 2019 - Towards a Resilient Built Environment - Risk and Asset Management. Guimarães, Portugal, pp 1734–1741
26. Lima DF (2022) Estruturas antigas de casquinha. Avaliação do impacto do caruncho pequeno por simulação da degradação. Master thesis, University of Minho
27. Derrick B, White P (2016) Why Welch's test is type I error robust. Quant Method Psychol 12:30–38
28. Denzler JK, Glos P (2007) Determination of shear strength values according to en 408. Mater Struct 40:79–86. https://doi.org/10.1617/s11527-006-9199-4
29. Grekin M, Surini T (2008) Shear strength and perpendicular-to-grain tensile strength of defect-free Scots pine wood from mature stands in Finland and Sweden. Wood Sci Technol 42:75–91. https://doi.org/10.1007/s00226-007-0151-8
30. EN 1995–1–1:2004. Eurocode 5–Design of timber structures–Part 1.1: General –Common rules and rules for buildings. European Committee for Standardization, Brussels